VIMS Articles   Virginia Institute of Marine Science

2017

Temporal progression of photosynthetic-strategy in phytoplankton in the Ross Sea, Antarctica

T. J. Ryan-Keogh

L. M. DeLizo
Virginia Institute of Marine Science

Walker O. Smith Jr.
Virginia Institute of Marine Science

et al

1 **Temporal progression of photosynthetic-strategy in**

2 **phytoplankton in the Ross Sea, Antarctica**

3

4 Thomas J. Ryan-Keogh[a1], Liza M. DeLizo[b], Walker O. Smith Jr.[b], Peter N. Sedwick[c],

5 Dennis J. McGillicuddy[d], C. Mark Moore[a] and Thomas S. Bibby[a]

6

7 [a]Ocean and Earth Science, University of Southampton, National Oceanography Centre,

8 Southampton, European Way, Southampton, SO14 3ZH, U.K.

9 Email: c.moore@noc.soton.ac.uk

10 Email: tsb@noc.soton.ac.uk

11 [b]Virginia Institute of Marine Sciences, The College of William and Mary, Gloucester

12 Point, Virginia, 23062, U.S.

13 Email: delizo@vims.edu

14 Email: wos@vims.edu

15 [c]Department of Ocean, Earth and Atmospheric Sciences, Old Dominion University,

16 Norfolk, Virginia, 23529, U.S.

17 Email: psedwick@odu.edu

18 [d]Applied Ocean Physics and Engineering, Woods Hole Oceanographic Institute,

19 Woods Hole, Massachusetts, 02543, U.S.

20 Email: mcgillic@whoi.edu

21

22 Author for correspondence email: Thomas.Ryan-Keogh@uct.ac.za

23

24

---

[1] Present address: Southern Ocean Carbon and Climate Observatory, CSIR - Natural Resources and the Environment, 15 Lower Hope Road, Rosebank, Cape Town, 7700, South Africa

Abstract

The bioavailability of iron influences the distribution, biomass and productivity of phytoplankton in the Ross Sea, one of the most productive regions in the Southern Ocean. We mapped the spatial and temporal extent and severity of iron-limitation of the native phytoplankton assemblage using long- (>24 h) and short-term (24 h) iron-addition experiments along with physiological and molecular characterisations during a cruise to the Ross Sea in December-February 2012. Phytoplankton increased their photosynthetic efficiency in response to iron addition, suggesting proximal iron limitation throughout most of the Ross Sea during summer. Molecular and physiological data further indicate that as nitrate is removed from the surface ocean the phytoplankton community transitions to one displaying an iron-efficient photosynthetic strategy characterised by an increase in the size of photosystem II (PSII) photochemical cross section (σ_{PSII}) and a decrease in the chlorophyll-normalised PSII abundance. These results suggest that phytoplankton with the ability to reduce their photosynthetic iron requirements are selected as the growing season progresses, which may drive the well-documented progression from *Phaeocystis antarctica*- assemblages to diatom-dominated phytoplankton. Such a shift in the assemblage-level photosynthetic strategy potentially mediates further drawdown of nitrate following the development of iron deficient conditions in the Ross Sea.

Keywords

Iron, Phytoplankton, Photosynthetic proteins, Photosystem II, Nutrient limitation, Ross Sea

Highlights

- Phytoplankton in the Ross Sea change their photosynthetic physiology over the growing season to a strategy requiring less iron.
- This results in fluorescence yields per chlorophyll and PSII both increasing as the growing season develops.
- This observation may help explain the well characterised seasonal progression from to *Phaeocystis* spp. to diatom spp. over the growing season and also have implications for the assessment of primary production from estimates of chlorophyll in this region.

1. Introduction

63

64   The Ross Sea continental shelf is the most productive region in the Southern
65 Ocean (Arrigo and van Dijken, 2004; Peloquin and Smith, 2007), with an annual
66 productivity >200 g C m^{-2} (Smith et al., 2006), which may account for as much as 27%
67 of the estimated total Southern Ocean biological CO_2 uptake (Arrigo et al., 2008). An
68 understanding of the controls on primary productivity is therefore needed given the
69 potential for future changes in stratification (Boyd et al., 2008; Smith et al., 2014) and
70 nutrient inputs to this region (Mahowald and Luo, 2003; Tagliabue et al., 2008).
71   A persistent polynya in the southern Ross Sea greatly increases in size in the
72 early austral spring (Arrigo and van Dijken, 2003; Reddy et al., 2007), and hosts large
73 seasonal phytoplankton blooms, typically dominated by the colonial haptophyte
74 *Phaeocystis antarctica* (*P. antarctica*) in spring through early summer (November –
75 December), with an increase in abundance of diatoms in mid- to late summer (Arrigo
76 and van Dijken, 2004; Arrigo et al., 1998; DiTullio and Smith, 1996; Goffart et al.,
77 2000; Smith and Gordon, 1997; Smith et al., 2000). Understanding the causes and
78 consequences of this seasonal phytoplankton progression is important, as the spatial
79 and temporal distribution and abundance of *P. antarctica* and diatoms have significant
80 biogeochemical consequences on, for example, the elemental composition and flux of
81 biogenic material from the euphotic zone (Arrigo et al., 1999; DeMaster et al., 1992;
82 Smith and Dunbar, 1998; Tagliabue and Arrigo, 2005).
83   Iron (Fe) and irradiance are assumed to exert the major 'bottom-up' controls on
84 phytoplankton biogeography and productivity in the Ross Sea, given the incomplete
85 macronutrient removal at the end of the growing season (Arrigo and van Dijken, 2003;
86 Arrigo et al., 1998; Coale et al., 2003; Fitzwater et al., 2000; Sedwick et al., 2000;
87 Sedwick et al., 2007; Smith et al., 2003; Smith et al., 2000; Tagliabue and Arrigo,
88 2003). Light availability may limit spring phytoplankton growth when vertical mixing
89 is deep and daily integrated irradiance is low, this mixing will also supply dissolved
90 iron (DFe) to the euphotic zone (McGillicuddy et al., 2015). As the growing season
91 progresses and the water column stratifies, the flux of DFe from below is likely reduced
92 and may therefore become a more significant factor in limiting phytoplankton growth
93 rates. Indeed, shipboard iron-addition experiments have repeatedly demonstrated the

94   role of iron limitation in the Ross Sea (Bertrand et al., 2007; Coale et al., 2003; Cochlan

95   et al., 2002; Martin et al., 1990; Olson et al., 2000; Sedwick and DiTullio, 1997;

96   Sedwick et al., 2000), consistent with other metrics of Fe stress including high levels

97   of flavodoxin (Maucher and DiTullio, 2003) and enhanced biological drawdown of

98   silicate relative to nitrate (Arrigo et al., 2000; Smith et al., 2006).

99   Changes in phytoplankton composition from *P. antarctica* to diatom species

100 may be linked to the co-limitation and interaction between iron and light. Boyd (2002)

101 speculated that *P. antarctica* growth is limited by Fe availability from spring through

102 late summer. Sedwick et al. (2007) further proposed that decreases in iron availability

103 through spring are mitigated by increases in irradiance, thereby decreasing

104 phytoplankton iron requirements. The differences in intracellular iron requirements

105 alongside changes in the light environment may explain the community succession of

106 the Ross Sea, where diatoms can outcompete *P. antarctica* in the late summer (Strzepek

107 et al., 2012).

108   Phytoplankton that dominate in the Ross Sea may therefore need to be adapted

109 to highly variable iron concentrations and light availability (Sedwick et al., 2011). An

110 antagonistic relationship between irradiance and photosynthetic Fe demand may be

111 predicted given that lower irradiances can increase Fe requirements associated with the

112 synthesis of the additional photosynthetic units required to increase light absorption

113 (Maldonado et al., 1999; Raven, 1990; Sunda and Huntsman, 1997). Each

114 photosynthetic electron transfer chain requires 22-23 Fe atoms, and the photosynthetic

115 apparatus can be the largest sink of Fe within a phytoplankton cell (Raven, 1990; Shi

116 et al., 2007; Strzepek and Harrison, 2004). In contrast to the tight link between cellular

117 Fe requirements and light harvesting capacity, studies on Southern Ocean diatoms and

118 *P. antarctica* in culture suggest the Fe burden of photosynthesis may be significantly

119 reduced for these species through increases in the size rather than the number of

120 photosynthetic units (termed sigma-type acclimation) in response to iron/ and light

121 limitation (Strzepek et al., 2012; Strzepek et al., 2011). Effectively, these Southern

122 Ocean taxa appear to invest relatively more resources in the generation of a larger light-

123 harvesting apparatus, rather than in the Fe-rich photosynthetic catalysts of

124 photosystems I and II (Strzepek et al., 2012). This Fe-efficient strategy appears to be

125 most pronounced for Southern Ocean diatoms, which, in culture can have some of the

126 largest light harvesting antennae reported (Strzepek et al., 2012), a phenotype which is

127 more commonly associated with small cells (Suggett et al., 2009). The photosynthetic

strategy of Southern Ocean diatoms may therefore contribute to the apparently low Fe requirement and cellular Fe:C ratio of these species (Coale et al., 2003; Kustka et al., 2015; Sedwick et al., 2007; Strzepek et al., 2012; Strzepek et al., 2011), and as such drive the seasonal progression from *P. antarctica* to diatoms in the Ross Sea.

In December-February 2012 a research cruise was conducted as part of the multidisciplinary research project *Processes Regulating Iron Supply at the Mesoscale – Ross Sea* (PRISM-RS), in an effort to identify and quantify the major sources of iron to the surface waters of the Ross Sea during the growing season. As part of this study, physiological and molecular measurements were combined with shipboard incubation experiments in an effort to define the spatial and temporal extent of phytoplankton iron limitation and reveal the photosynthetic strategy of the phytoplankton assemblages.

2. Materials and Methods

2.1. Oceanographic Sampling

The samples and data presented here were obtained during a cruise of the *RVIB Nathaniel B. Palmer* to the Ross Sea (cruise NBP12-01) from 24th December 2011 to 10th February 2012 (DOY 358 – 041). During the cruise, 29 short-term (24 h) and 3 long-term (168 h) incubation experiments were performed (Fig. 1a). Short-term experiments were used to determine rapid iron induced changes in the phytoplankton photophysiological status; whereas long-term experiments determined whether relief from iron limitation could drive changes in biomass. For the long-term incubation experiments, uncontaminated whole seawater was collected from ~5 m depth whilst slowly underway, using a trace-metal clean towed fish system (Sedwick et al., 2011). Uncontaminated whole seawater for the short-term incubation experiments was collected from ~10 m depth in Teflon-lined, external closure 5 L Niskin-X samplers (General Oceanics) deployed on a trace metal clean CTD rosette system (Marsay et al., 2014). Samples for additional analysis were also collected along the cruise track.

2.2. Bioassay Incubation Experiments

Incubation experiments were performed using methods similar to those employed previously in the Southern Ocean (Moore et al., 2007; Nielsdóttir et al., 2012) and the high latitude North Atlantic (HLNA) (Nielsdóttir et al., 2009; Ryan-Keogh et al., 2013). Water for the experiments (see 2.1, above) was transferred unscreened into acid-washed 1.0-L polycarbonate bottles (Nalgene) for the short-term incubation experiments and 4.5-L polycarbonate bottles for the long-term incubation experiments. Incubation bottles were filled in a random order, with triplicate samples for initial measurements in the long-term incubation experiments collected at the beginning, middle and end of the filling process. Initial samples for the short-term incubation experiments were collected from the same Niskin-X sampling bottle. The short-term experiments were run for 24 h and the long-term experiments were run for 168 h; both experiments consisted of two treatments: an unamended control treatment and 2.0 nmol L^{-1} Fe

171 treatment (hereafter, + Fe). All experimental incubations were conducted as biological

172 duplicates or triplicates.

173   All bottle tops were externally sealed with film (Parafilm™), and bottles were

174 double bagged with clear polyethylene bags to minimize risks of contamination during

175 the incubation. On-deck incubators were shaded using LEE "blue lagoon" filters to

176 provide light levels corresponding to ~35% of above-surface irradiance (Hinz et al.,

177 2012; Nielsdóttir et al., 2009; Ryan-Keogh et al., 2013). Flowing surface seawater was

178 used to control the temperature in the incubators. Subsampling of long-term incubations

179 for measurements of chlorophyll *a*, dissolved macronutrient concentrations and

180 phytoplankton physiological parameters occurred after 24, 72, 120 and 168 h. Sub-

181 sampling of short-term incubation experiments for the same parameters occurred after

182 24 h. All experiments were set up and sub-sampled under a class-100 laminar flow hood

183 within a trace metal clean environment.

184

185   2.3. Chlorophyll *a* and Nutrient Analysis

186

187 Samples for chlorophyll *a* (Chl) analysis (250 mL) were filtered onto GF/F filters and

188 then extracted into 90% acetone for 24 h in the dark at 4°C, followed by analysis with

189 a fluorometer (TD70; Turner Designs) (Welschmeyer, 1994). Macronutrient samples

190 were drawn into 50 mL diluvials and refrigerated at 4°C until analysis, which typically

191 commenced within 12 h of sampling. Nitrate plus nitrite (DIN), phosphate, ammonium

192 and silicate were determined shipboard on a five-channel Lachat Instruments

193 QuikChem FIA+ 8000s series AutoAnalyser (Armstrong et al., 1967; Atlas et al., 1971;

194 Bernhardt and Wilhelms, 1967; Patton, 1983). Dissolved iron was determined post-

195 cruise using flow injection analysis modified from Measures et al. (1995), as described

196 by Sedwick et al. (2011); accuracy of the DFe method was verified by analysis of SAFe

197 reference seawater samples (Johnson et al., 2007).

198

199   2.4. Phytoplankton Photosynthetic Physiology

200

201 Variable chlorophyll fluorescence was measured using a Chelsea Scientific Instruments

202 Fastracka™ Mk II Fast Repetition Rate fluorometer (FRRf) integrated with a FastAct™

203 Laboratory system. All samples were acclimated in opaque bottles for 30 minutes at *in*

204 *situ* temperatures, and FRRf measurements were blank corrected effect using carefully

205   prepared 0.2 μm filtrates for all samples (Cullen and Davis, 2003). Blanks were

206   typically around 1% and always <10% of the maximum fluorescence signal. Protocols

207   for FRRf measurements and data processing were similar to those detailed elsewhere

208   (Moore et al., 2007). Data from the FRRf were analysed to derive values of the

209   minimum and maximum fluorescence (F_o and F_m) and hence F_v/F_m (where $F_v = F_m -$

210   F_o), as well as the functional absorption cross-section of PSII (σ_{PSII}) by fitting transients

211   to the model of Kolber et al. (1998).

212

213   2.5. Phytoplankton Composition

214

215   Samples for photosynthetic pigment analysis were collected and measured by high

216   performance liquid chromatography (HPLC). 0.3 − 1.0 L of sea-water were filtered

217   through GF/F filters, which were immediately flash frozen in liquid nitrogen and stored

218   at -80°C until analysis. Pigments were extracted into 90% acetone by sonication

219   before quantification using a Waters Spherisorb ODSU C-18 HPLC column and Waters

220   HPLC system as described in Smith et al. (2006). Algal community composition was

221   then estimated from pigment concentrations following the method of Arrigo et al.

222   (1999).

223

224   2.6. Total Protein Extraction and Quantification

225

226   Photosynthetic protein abundances were quantified using techniques similar to those

227   described elsewhere (Brown et al., 2008; Macey et al., 2014; Ryan-Keogh et al., 2012).

228   Samples for protein extraction were collected by filtering 1.0-3.0 L of seawater onto

229   GF/F filters (Whatman) under low light for ~45 minutes to minimize changes in protein

230   abundance following sampling. Filters were flash frozen and stored at -80°C until

231   analysis. Proteins were extracted in the laboratory according to the protocol described

232   by Brown et al. (2008). Quantification was performed using custom Agrisera™ primary

233   antibodies and peptide standards, which were designed against peptide tags conserved

234   across all oxygenic photosynthetic species for protein subunits that are representative

235   of the functional photosynthetic complex PsbA (PSII) (Campbell et al., 2003). Protein

236   abundances were quantified using QuantityOne™ and ImageLab™ software;

237   quantification was performed within the unsaturated portion of the calibration curve.

238   The estimated protein abundances were comparable to those reported for natural

239   phytoplankton communities using similar methods (Hopkinson et al., 2010; Losh et al.,

240   2013; Macey et al., 2014; Richier et al., 2012).

241

3. Results and Discussion

3.1. General Oceanography

A range of oceanographically distinct regions was occupied on the Ross Sea continental shelf during the PRISM-RS cruise (Fig. 1). These included areas close to the Ross Ice Shelf, near and within pack ice, and over shallow bathymetric features, both of which may provide important sources of DFe to the upper water column (McGillicuddy et al., 2015). Highest chlorophyll a concentrations (Fig. 2a) were associated with the ice-shelf in the southwestern Ross Sea (24.6 μg Chl L^{-1}) and correlated with the lowest DIN (dissolved inorganic nitrate + nitrite) concentrations (Figs. 2b, 3) and lowest surface F_v/F_m values observed (Figs. 2c, 3). Surface DFe concentrations ranged from 0.067-0.787 nM (Fig. 2d), were not correlated with chlorophyll or DIN concentrations (Fig. 3, Supplementary Information, Fig. S1), and were elevated off the continental shelf in the northeast sector of the Ross Sea.

3.2. Mapping of Iron Limitation

Despite being the most productive region in the Southern Ocean, our results confirm that phytoplankton growth in the Ross Sea is limited by iron availability during summer, consistent with previous studies (Bertrand et al., 2011; Bertrand et al., 2007; Coale et al., 2003; Cochlan et al., 2002; Martin et al., 1990; Olson et al., 2000; Sedwick and DiTullio, 1997; Sedwick et al., 2000). The response of phytoplankton to iron-addition was assayed through a series of long- (168 h) and short-term (24 h) iron-addition incubations (Fig. 1), while no clear spatial pattern in iron stress could be observed from a single cruise during a time of relatively rapid changes in a spatio-temporally complex system (Fig. 2), there was evidence of an increase in photosynthetic efficiency following iron addition throughout much of the Ross Sea during summer, highlighting the role of iron in influencing phytoplankton physiology. To compare these iron-mediated changes in F_v/F_m, $\Delta(F_v/F_m)$ was calculated as defined in Ryan-Keogh et al. (2013), as the difference between the Fe-amended and control treatments (Equation 1).

275   Equation 1 Calculation of $\Delta(F_v/F_m)$.

276      $$\Delta\left(F_v/F_m\right) = \frac{F_v/F_{m+Fe} - F_v/F_{m\,Control}}{Time}$$

277   Values of $\Delta(F_v/F_m)$ were frequently positive following iron addition (ranging from 0.00

278   - 0.17) (Fig. 4a), suggesting that Fe amendments increased the photosynthetic

279   efficiency of phytoplankton in much of the Ross Sea during the sampling period.

280   Data from long-term (168 h) experiments (Table 1 and Fig. 4) enable a more

281   detailed analysis of the response of phytoplankton to iron-additions. Three experiments

282   were initiated from (1) near the Ross Ice Shelf, (2) over the Ross Bank and (3) in an

283   anti-cyclonic eddy (Figs. 1 and 4). The three experiments revealed varying responses

284   to iron additions by the extant phytoplankton assemblage. Experiments 1 and 3 gave a

285   strong and positive response to iron additions, and provided evidence that

286   phytoplankton were iron limited. Shorter-term responses revealed elevated values of

287   F_v/F_m (i.e., a positive $\Delta(F_v/F_m)$) after 24 h (Fig. 4a), with subsequent significant

288   (ANOVA, $p<0.05$) increases in growth rates and nutrient removal observed after 168 h

289   (Table 1). Experiment 2, initiated over the Ross Bank, did not show an increase in

290   photosynthetic efficiency $\Delta(F_v/F_m)$ (Fig. 4a). Moreover, growth rate and nutrient

291   removal were not significantly different between control and iron-addition conditions

292   until after >168 h (ANOVA, $p>0.05$) (Table 1), which most likely reflects severe

293   depletion of ambient DFe in the control treatments by this time. The Ross Bank (Fig.

294   4a, Table 1) has a shallow bathymetry (~150 m), and none of the Fe-addition

295   experiments in this region showed a significant response (Fig. 4). The Ross Bank may

296   therefore provide significant and continuous DFe inputs to the euphotic zone, thereby

297   ultimately stimulating productivity.

298   The measurement of F_v/F_m is derived from analysis of the fluorescence kinetics

299   emitted from the photosynthetic reaction centre photosystem II (PSII) and its associated

300   light-harvesting antenna (Kolber and Falkowski, 1993). Understanding the mechanism

301   of changes to F_v/F_m can provide information on the process by which phytoplankton

302   respond to iron-limitation. Absolute changes in maximum fluorescence (F_m) and

303   variable fluorescence (F_v) normalised to chlorophyll *a* were calculated (Figs. 4b and c),

304   revealing a significant difference between the +Fe and control treatments in F_m Chl^{-1} (t

305   = 24 h (*t*-test, $p<0.05$)), whereas there was no significant difference for F_v Chl^{-1} (t = 24

306   h (*t*-test, $p>0.05$)). This suggests that changes in F_v/F_m reflect changes in the proportion

307   of chlorophyll that is photosynthetically coupled to active PSII reaction centres, rather

13

308 than changes in the activity of PSII (Behrenfeld et al., 2006; Lin et al., 2016; Macey et

309 al., 2014).   A similar response was observed for all short-term iron-addition

310 experiments that exhibited positive changes in $\Delta(F_v/F_m)$.

311

312 3.3 Temporal Development of Photosynthetic Strategy

313

314 Given the high degree of spatial variability in response to iron-additions, we placed all

315 observations within a unified framework, hence producing a conceptualised model of

316 temporal progression of phytoplankton within the Ross Sea. The PRISM-RS cruise

317 sampled for 30 days covering a period from mid- to late summer, during which we

318 expected iron limitation of phytoplankton growth to be significant (Sedwick et al.,

319 2000). Total phytoplankton biomass accumulation is dependent on growth after the

320 sampled regions become ice-free (Arrigo and van Dijken, 2003) and the losses due to

321 grazing, sinking and physical removal. All spatial data therefore represent a mosaic of

322 different temporal progressions that represent different stages of phytoplankton

323 development. We utilise surface nitrate (DIN) as a proxy to separate the temporal

324 patterns from any spatial differences (Fig. 5). As phytoplankton biomass (Chl)

325 increased, nutrients were removed and F_v/F_m reduced (Figs. 3, 5a).   Pigment data

326 showed that the nutrient drawdown and Chl increase in parallel with a shift from *P.*

327 *antarctica*-dominated to diatom-dominated assemblages (Figs. 3, 5b).   Within this

328 conceptual framework, the relative severity of Fe-stress ($\Delta F_v/F_m$) may be inferred from

329 the Fe-addition incubation experiments.   Two potential phases of Fe deficiency were

330 identified (Fig. 5c): first, when DIN concentrations remain high (> ~20 µM) and *P.*

331 *antarctica* is a major component of the phytoplankton (labelled '1'), and secondly when

332 DIN is further removed (to < ~20 µM) by diatom-dominated communities (labelled '2';

333 Fig. 5c).

334   Photophysiological parameters are presented within this framework. The

335 relative size of the effective light-harvesting cross-section of PSII (σ_{PSII}) (Fig. 6a) is

336 low (~1.6 nm^{-2}) when DIN and F_v/F_m are high, and approximately doubles to ~3.29 nm^{-}

337 ^{2} as DIN is depleted and the assemblage becomes diatom-dominated. Quantification of

338 the photosynthetic catalyst PSII further characterises the photosynthetic strategy of

339 phytoplankton in the Ross Sea. Chlorophyll normalised to abundances of the protein

340 target PsbA (indicative of the abundance of PSII; (Brown et al., 2008) (Chl:PsbA),

341 which can provide another indication of the relative sizes of the light harvesting

pigment antenna relative the abundance of the photosystems, is lower at higher DIN concentrations and increases as DIN and F_v/F_m decrease (Fig. 6b). Combining the protein abundance data and the photophysiological measurements, the maximum fluorescent yield per chlorophyll (F_m:Chl) (Fig. 6c) and per PSII (F_m:PsbA) (Fig. 6d) can also be calculated. Both of these parameters increase, by 46 and 296% respectively, with decreases in DIN and F_v/F_m.

Together, these photophysiological measurements and corresponding environmental information at the time of sampling therefore indicate several significant correlations (Fig. 3 & Supplementary Information, S1) associated with the potential drivers of the observed transition in community structure and subsequent changes in photophysiology. Thus, within our conceptual frame work, using DIN concentration as a proxy for the stage of the phytoplankton bloom, we observe statistically significant positive correlations ($p<0.01$) with other macronutrients and the photosynthetic efficiency (F_v/F_m) which all decline as nitrate is removed from the system. While negative correlations ($p<0.01$) are observed between DIN and temperature, chlorophyll concentration, the relative abundance of diatoms and σ_{PSII} which all increase as nitrate is removed from the system. While no significant correlation is seem between DIN and the fluorescence yield per PSII (F_m:PSII) or the chlorophyll content per PSII (Chl:PSII), there is a significant negative correlation between F_m:Chl and PSII:Chl ($p<0.01$) (Fig. 3).

No statistically significant ($p<0.01$) relationships were observed with dissolved iron concentrations, suggesting that this variable may not represent a good indicator of iron stress, as might be expected considering that any limiting nutrient would be expected to be severely depleted by biological uptake. Overall, the observed correlations are thus taken to be indicative of the phytoplankton community transitioning between dominant groups as SST increases, non-limiting macronutrients are drawn down and the community biomass increases, potential as a result of different Fe utilisation capacities between diatoms and *P. antarctica* (Strzepek et al., 2012). These observations may also support that the hypothesis that Southern Ocean diatoms may both acquire (Kustka et al., 2015) and utilise (Strzepek et al., 2012) iron more effectively than *P. antarctica* and that the community transition may enable further drawdown of nitrate.

While there can be an array of reasons for diatoms being better at acquiring and utilising available DFe as it becomes limiting during summer in the Ross Sea, differences in photosynthetic strategy have the potential to be a significant factor in

376   regulating the temporal changes that occur, given that the photosynthetic apparatus

377   represents the dominant sink for Fe in a phytoplankton cell (Raven, 1990; Strzepek and

378   Harrison, 2004). The analysis presented here clearly demonstrates that a different

379   photosynthetic strategy is apparent within the phytoplankton community responsible

380   for the initial DIN removal vs. those responsible for the later DIN removal. These

381   observations of photosynthetic strategy are consistent with some of the

382   ecophysiological differences observed within culture-based studies of Southern Ocean

383   phytoplankton (Strzepek et al., 2012). Phytoplankton in the Ross Sea generally display

384   a large, functional light-harvesting cross section for PSII (σ_{PSII}) compared to temperate

385   species (Smith et al., 2011). As has been proposed (Strzepek et al., 2012), this may

386   reflect a strategy by which cells acclimate and/or adapt through increasing the size of

387   photosynthetic units rather than the number of photosynthetic units in a low Fe

388   environment – thus escaping the typical antagonistic relationship between iron-demand

389   and light capture (Sunda and Huntsman, 1997). Our measurements of the abundance

390   of the photosynthetic catalysis PSII were also consistent with such an observation,

391   whereby the increase in the ratio of Chl:PSII mirrors the increase in σ_{PSII}. (Fig. 6b).

392   This strategy could significantly reduce the iron-demand normally associated with the

393   photosynthetic apparatus. Phytoplankton that dominate at low DIN have a particularly

394   large σ_{PSII} and have increased Chl:PSII values by 255%, again in agreement with culture

395   studies in which Southern Ocean diatoms have larger σ_{PSII} than *P. antarctica* (Strzepek

396   et al., 2012).

397   We thus suggest that the diatoms that dominate in summer as DIN is removed may

398   represent a refined strategy to reduced iron availability, noting that previous

399   information from temperate taxa and regions (Suggett et al., 2009) would tend to

400   suggest that relatively high functional cross sections would be unlikely in

401   phytoplankton with large cell sizes typical of many Southern Ocean diatoms (Suggett

402   et al., 2009). Large cells with large σ_{PSII} may, however, result in ecophysiological trade-

403   offs, including a tendency for over-excitation of PSII and photodamage, which may

404   require a rapid PSII repair cycle or a requirement for rapidly inducible and significant

405   non-photochemical quenching (Campbell and Tyystjärvi, 2012; Petrou et al., 2010; Wu

406   et al., 2011), possibly suggesting Antarctic diatoms would require novel

407   photoprotective strategies. Despite these potential negative consequences of a large

408   σ_{PSII}, Antarctic diatoms seem to have adopted a phenotypic response underlining the

409 relevance of iron-availability and providing some explanation for the low Fe:C ratios
410 in some of these species (Strzepek et al., 2012).

411 While the observations in this study were restricted to the summer season they
412 do include DIN concentrations similar to those estimated for the winter mixed layer
413 nitrate concentration (McGillicuddy et al., 2015) and so potentially conditions
414 analogous to a broader seasonal progression in phytoplankton composition in the Ross
415 Sea from *P. antarctica* early in the growing season to diatom-dominance later in
416 summer (Smith et al., 2010). The dataset therefore provides indications of potential
417 contributory mechanisms for this seasonal progression, while also reflecting the large
418 degree of spatial heterogeneity in physical and biological processes throughout the
419 growing season in the Ross Sea (Smith and Jones, 2015).

420 The data presented here also provide insights into the mechanism of the iron-
421 stress response of phytoplankton. Increases in F_v/F_m are commonly reported as a
422 response to Fe addition (Boyd et al., 2008; Feng et al., 2010). Results from the
423 experiments and observations show that increases in F_v/F_m in response to Fe addition
424 and elevated F_v/F_m values in regions with modest DIN drawdown result from reduction
425 in the ratio of F_m:Chl (or F_m:PSII) rather than changes in F_v:Chl. This is in agreement
426 with similar observations from the high latitude North Atlantic and Equatorial Pacific
427 (Behrenfeld et al., 2006; Lin et al., 2016; Macey et al., 2014) regions and implies that
428 low F_v/F_m results from changes in the coupling of light-harvesting chlorophyll-binding
429 proteins to photosynthesis rather than accumulation of damaged photosystems. Such
430 accumulation of non-photosynthetically active chlorophyll-binding proteins in Fe-
431 limited oceanic regions can have consequences on estimates of productivity in these
432 regions (Behrenfeld et al., 2006).

4. Conclusions

The current study represents an analysis of the summer photosynthetic strategies of phytoplankton in the Ross Sea and highlights how different iron-efficiency strategies occur in phytoplankton as Fe becomes limiting and irradiance availability becomes maximal. This is important for understanding Fe usage efficiency in the region. The Ross Sea clearly differs from other high latitude regions due to plankton composition, yet iron availability still contributes to reduced growth rates and macronutrient removal. Even though this system is one of the most productive regions in the Southern Ocean, iron availability still exerts a strong control over summer productivity and biomass accumulation, and any changes in future iron supply induced by climate change could have profound effects. Climate-mediated changes to the mixed layer depth and sea-ice cover could change iron limitation strategies and phytoplankton phenology (Boyd et al., 2012), as well as alterations to iron supply from highly variable supply mechanisms such as Australian and local dust inputs (Mackie et al., 2008). The Southern Ocean is predicted to be particularly biogeochemically significant with respect to climate change (Marinov et al., 2006) and is the only iron-limited HNLC region where the cryosphere plays a major role. An understanding of the role of iron limitation in this highly dynamic environment is thus particularly important; particularly as climate mediated variability is expected to increase.

5. References

Armstrong, F.A.J., Stearns, C.R., Strickland, J.D.H., 1967. The measurement of upwelling and subsequent biological processes by means of the Technicon AutoAnalyzer and associate equipment. Deep-Sea Research 14, 381-389.

Arrigo, K.R., DiTullio, G.R., Dunbar, R.B., Robinson, D.H., VanWoert, M., Worthen, D.L., Lizotte, M.P., 2000. Phytoplankton taxonomic variability in nutrient utilization and primary production in the Ross Sea. J Geophys Res 105, 8827-8845.

Arrigo, K.R., Robinson, D.H., Worthen, D.L., Dunbar, R.B., DiTullio, G.R., VanWoert, M., Lizotte, M.P., 1999. Phytoplankton community structure and the drawdown of nutrients and CO_2 in the Southern Ocean. Science 283, 365-367.

Arrigo, K.R., van Dijken, G.L., 2003. Phytoplankton dynamics within 37 Antarctic coastal polynya systems. J Geophys Res 108, 3271.

Arrigo, K.R., van Dijken, G.L., 2004. Annual changes in sea-ice, chlorophyll a, and primary production in the Ross Sea, Antarctica. Deep-Sea Research II 51, 117-138.

Arrigo, K.R., van Dijken, G.L., Long, M., 2008. Coastal Southern Ocean: A strong anthropogenic CO_2 sink. Geophysical Research Letters 35, L21602.

Arrigo, K.R., Worthen, D., Schnell, A., Lizotte, M.P., 1998. Primary production in Southern Ocean waters. J Geophys Res 103, 15587-15600.

Atlas, e.l., Hager, S.W., Gordon, L.I., Park, P.K., 1971. A practical manual for use of the Technicon Autoanalyzer in seawater nutrient analyses: revised, Technical Report 215. Oregon State University, p. 48.

Behrenfeld, M.J., Worthington, K., Sherrell, R.M., Chavez, F.P., Strutton, P., McPhaden, M., Shea, D.M., 2006. Controls on tropical Pacific Ocean productivity revealed through nutrient stress diagnostics. Nature 442, 1025-1028.

Bernhardt, H., Wilhelms, A., 1967. The continuous determination of low level iron, soluble phosphate and total phosphate with the AutoAnalyzer, Technicon Symposium, p. 386.

Bertrand, E.M., Saito, M.A., Lee, P.A., Dunbar, R.B., Sedwick, P.N., Ditullio, G.R., 2011. Iron limitation of a springtime bacterial and phytoplankton community in the Ross Sea: implications for vitamin b(12) nutrition. Frontiers in microbiology 2, 160.

491   Bertrand, E.M., Saito, M.A., Rose, J.M., Riesselman, C.R., Lohan, M.C., Noble, A.E.,

492   Lee Peter, A., DiTullio, G.R., 2007. Vitamin B12 and iron co-limitation of

493   phytoplankton growth in the Ross Sea. Limnol Oceanogr 52, 1078-1093.

494   Boyd, P.W., 2002. Environmental factors controlling phytoplankton processes in the

495   Southern Ocean. J Phycol 38, 844-861.

496   Boyd, P.W., Arrigo, K.R., Strzepek, R., van Dijken, G.L., 2012. Mapping

497   phytoplankton iron utilization: Insights into Southern Ocean supply mechanisms. J

498   Geophys Res 117, C06009.

499   Boyd, P.W., Doney, S.C., Strzepek, R., Dusenberry, J., Lindsay, K., Fung, I., 2008.

500   Climate-mediated changes to mixed-layer properties in the Southern Ocean: assessing

501   the phytoplankton response. Biogeosciences 5, 847-864.

502   Brown, C.M., MacKinnon, J.D., Cockshutt, A.M., Villareal, T.A., Campbell, D.A.,

503   2008. Flux capacities and acclimation costs in *Trichodesmium* from the Gulf of

504   Mexico. Marine Biology 154, 413-422.

505   Campbell, D.A., Cockshutt, A.M., Porankiewicz-Asplund, J., 2003. Analysing

506   photosynthetic complexes in uncharaterized species or mixed microalgal communities

507   using global antibodies. Physiol Plant 119, 322-327.

508   Campbell, D.A., Tyystjärvi, E., 2012. Parameterization of photosystem II

509   photoinactivation and repair. Biochim Biophys Acta 1817, 258-265.

510   Coale, K.H., Wang, X.J., Tanner, S.J., Johnson, K.S., 2003. Phytoplankton growth

511   and biological response to iron and zinc addition in the Ross Sea and Antarctic

512   Circumpolar Current along 170 degrees W. Deep-Sea Research II 50, 635-653.

513   Cochlan, W.P., Bronk, D.A., Coale, K.H., 2002. Trace metals and nitrogenous

514   nutrition of Antarctic phytoplankton: experimental observations in the Ross Sea.

515   Deep-Sea Research II 49, 3365-3390.

516   Cullen, J.J., Davis, R.F., 2003. The blank can make a big difference in oceanographic

517   measurements. Limnology and Oceanography Bulletin 12, 29-35.

518   DeMaster, D.j., Dunbar, R.B., Gordon, L.I., Leventer, A.R., Morrison, J.M., Nelson,

519   D.M., Nittrouer, C.A., Smith, W.O., Jr., 1992. Cycling and accumulation of biogenic

520   silica and organic matter in high-latitude environments: The Ross Sea. Oceanography

521   5, 146-153.

522   DiTullio, G.R., Smith, W.O., 1996. Spatial patterns in phytoplankton biomass and

523   pigment distributions in the Ross Sea. J Geophys Res 101, 18467-18477.

524   Feng, Y., Hare, C.E., Rose, J.M., Handy, S.M., DiTullio, G.R., Lee, P.A., Smith,

525   W.O., Jr., Peloquin, J., Tozzi, S., Sun, J., Zhang, Y., Dunbar, R.B., Long, M.C.,

526   Sohst, B., Lohan, M., Hutchins, D.A., 2010. Interactive effects of iron, irradiance and

527   CO_2 on Ross Sea phytoplankton. Deep-Sea Research I 57, 368-383.

528   Fitzwater, S.E., Johnson, K.S., Gordon, R.M., Coale, K.H., Smith, W.O., Jr., 2000.

529   Trace metal concentrations in the Ross Sea and their relationship with nutrients and

530   phytoplankton growth. Deep-Sea Research II 47, 3159-3179.

531   Goffart, A., Catalano, G., Hecq, J.H., 2000. Factors controlling the distribution of

532   diatoms and *Phaeocystis* in the Ross Sea. Journal of Marine Systems 27, 161-175.

533   Hinz, D.J., Nielsdóttir, M.C., Korb, R.E., Whitehouse, M.J., Poulton, A.J., Moore,

534   C.M., Achterberg, E.P., Bibby, T.S., 2012. Responses of microplankton community

535   structure to iron addition in the Scotia Sea. Deep-Sea Research II 59, 36-46.

536   Hopkinson, B.M., Xu, Y., Shi, D., McGinn, P.J., Morel, F.M.M., 2010. The effect of

537   CO_2 on the photosynthetic physiology of phytoplankton in the Gulf of Alaska. Limnol

538   Oceanogr 55, 2011-2024.

539   Johnson, K.S., Elrod, V.A., Fitzwater, S.E., Plant, J., Boyle, E., Bergquist, B.,

540   Bruland, K.W., Aguilar-Islas, A.M., Buck, K., Lohan, M.C., Smith, G.J., Sohst, B.M.,

541   Coale, K.H., Gordon, M., Tanner, S., Measures, C.I., Moffett, J., Barbeau, K.A.,

542   King, A., Bowie, A.R., Chase, Z., Cullen, J.J., Laan, P., Landing, W., Mendez, J.,

543   Milne, A., Obata, H., Doi, T., Ossiander, L., Sarthou, G., Sedwick, P.N., Van den

544   Berg, S., Laglera-Baquer, L., Wu, J.-F., Cai, Y., 2007. Developing standards for

545   dissolved iron in seawater. Eos, Transactions American Geophysical Union 88, 131-

546   132.

547   Kolber, Z.S., Falkowski, P.G., 1993. Use of active fluorescence to estimate

548   phytoplankton photosynthesis in situ. Limnol Oceanogr 38, 1646-1665.

549   Kolber, Z.S., Prášil, O., Falkowski, P.G., 1998. Measurements of variable chlorophyll

550   fluorescence using fast repetition rate techniques: defining methodology and

551   experimental protocols. Biochim Biophys Acta 1367, 88-106.

552   Kustka, A.B., Jones, B.M., Hatta, M., Field, M.P., Milligan, A.J., 2015. The influence

553   of iron and siderophores on eukaryotic phytoplankton growth rates and community

554   composition in the Ross Sea. Mar Chem 173, 195-207.

555   Lin, H., Kuzimov, F.I., Park, J., Lee, S., Falkowski, P.G., Gorbunov, M.Y., 2016. The

556   fate of photons absorbed by phytoplankton in the global ocean. Science 351, 264-267.

557   Losh, J.L., Young, J.N., Morel, F.M.M., 2013. Rubisco is a small fraction of total

558   protein in marine phytoplankton. New Phytol 198, 52-58.

559   Macey, A.I., Ryan-Keogh, T.J., Richier, S., Moore, C.M., Bibby, T.S., 2014.

560   Photosynthetic protein stoichiometry and photophysiology in the high latitude North

561   Atlantic. Limnol Oceanogr 59, 1853-1864.

562   Mackie, D.S., Boyd, P.W., McTainsh, G.H., Tindale, N.W., Westberry, T.K., Hunter,

563   K.A., 2008. Biogeochemistry of iron in Australian dust: From eolian uplift to marine

564   uptake. Geochemistry, Geophysics, Geosystems 9, Q03Q08.

565   Mahowald, N.M., Luo, C., 2003. A less dusty future? Geophysical Research Letters

566   30, 1903 doi:1910.1029/2003GL917880.

567   Maldonado, M.T., Boyd, P.W., Harrison, P.J., Price, N.M., 1999. Co-limitation of

568   phytoplankton growth by light and Fe during winter in the NE subarctic Pacific

569   Ocean. Deep-Sea Research II 46, 2475-2485.

570   Marinov, I., Gnanadesikan, A., Toggweiler, J.R., Sarmiento, J.L., 2006. The Southern

571   Ocean biogeochemical divide. Nature 441, 964-967.

572   Marsay, C.M., Sedwick, P.N., Dinniman, M.S., Barrett, P.M., Mack, S.L.,

573   McGillicuddy, D.J., 2014. Estimating the benthic efflux of dissolved iron on the Ross

574   Sea continental shelf. Geophysical Research Letters 41, 7576-7583.

575   Martin, J.H., Gordon, R.M., Fitzwater, S.E., 1990. Iron in Antarctic waters. Nature

576   345, 156-158.

577   Maucher, J.M., DiTullio, G.R., 2003. Flavodoxin as a diagnostic indicator of chronic

578   iron limitation in the Ross Sea and New Zealand sector of the Southern Ocean,

579   Biogeochemistry of the Ross Sea. American Geophysical Union, Washington D.C.,

580   pp. 35-52.

581   McGillicuddy, D.J., Sedwick, P.N., Dinniman, M.S., Arrigo, K.R., Bibby, T.S.,

582   Greenan, B.J.W., Hofmann, E.E., Klinck, J.M., Smith, W.O., Jr., Mack, S.L., Marsay,

583   C.M., Sohst, B.M., van Dijken, G.L., 2015. Iron supply and demand in an Antarctic

584   shelf ecosystem. Geophysical Research Letters.

585   Measures, C.I., Yuan, J., Resing, J.A., 1995. Determination of iron in seawater by

586   flow injection analysis using in-line preconcentration and spectrophotometric

587   detection. Mar Chem 50, 3-12.

588   Moore, C.M., Seeyave, S., Hickman, A.E., Allen, J.T., Lucas, M.I., Planquette, H.,

589   Pollard, R.T., Poulton, A.J., 2007. Iron-light interactions during the CROZet natural

iron bloom and EXport experiment (CROZEX) I: Phytoplankton growth and

photophysiology. Deep-Sea Research II 54, 2045-2065.

Nielsdóttir, M.C., Bibby, T.S., Moore, C.M., Hinz, D.J., Sanders, R., Whitehouse, M.,

Korb, R., Achterberg, E.P., 2012. Seasonal and spatial dynamics of iron availability in

the Scotia Sea. Mar Chem 130, 62-72.

Nielsdóttir, M.C., Moore, C.M., Sanders, R., Hinz, D.J., Achterberg, E.P., 2009. Iron

limitation of the postbloom phytoplankton communities in the Iceland Basin. Global

Biogeochemical Cycles 23, 1-13.

Olson, R.J., Sosik, H.M., Chekalyuk, A.M., Shalapyonok, A., 2000. Effects of iron

enrichment on phytoplankton in the Southern Ocean during late summer: active

fluorescence and flow cytometric analyses. Deep-Sea Research II 47, 3181-3200.

Patton, C.J., 1983. Design, characterization and applications of a miniature continous

flow analysis system. Michigan State University, Ann Arbor, Michigan.

Peloquin, J.A., Smith, W.O., Jr., 2007. Phytoplankton blooms in the Ross Sea,

Antarctica: Interannual variability in magnitude, temporal patterns, and composition. J

Geophys Res 112, C08013.

Petrou, K., Hill, R., Brown, C.M., Campbell, D.A., Doblin, M.A., Ralph, P.J., 2010.

Rapid photoprotection in sea-ice diatoms from the East Antarctic pack ice. Limnol

Oceanogr 55, 1400-1407.

Raven, J.A., 1990. Predictions of Mn and Fe use efficiencies of phototrophic growth

as a function of light availability for growth and C assimilation pathway. New Phytol

116, 1-18.

Reddy, T.E., Arrigo, K.R., Holland, D.M., 2007. The role of thermal and mechanical

processes in the formation of the Ross Sea summer polynya. J Geophys Res 112.

Richier, S., Macey, A.I., Pratt, N.J., Honey, D.J., Moore, C.M., Bibby, T.S., 2012.

Abundances of Iron-Binding Photosynthetic and Nitrogen-Fixing Proteins of

Trichodesmium Both in Culture and In Situ from the North Atlantic. Plos One 7,

e35571.

Ryan-Keogh, T.J., Macey, A.I., Cockshutt, A.M., Moore, C.M., Bibby, T.S., 2012.

The cyanobacterial chlorophyll-binding-protein IsiA acts to increase the *in vivo*

effective absorption cross-section of photosystem I under iron limitation. J Phycol 48,

145-154.

Ryan-Keogh, T.J., Macey, A.I., Nielsdóttir, M., Lucas, M.I., Steigenberger, S.S.,

Stinchcombe, M.C., Achterberg, E.P., Bibby, T.S., Moore, C.M., 2013. Spatial and

624 temporal development of phytoplankton iron stress in relation to bloom dynamics in

625 the high-latitude North Atlantic Ocean. Limnol Oceanogr 58, 533-545.

626 Sedwick, P.N., DiTullio, G.R., 1997. Regulation of algal blooms in Antarctic shelf

627 waters by the release of iron from melting sea ice. Geophysical Research Letters 24,

628 2515-2518.

629 Sedwick, P.N., DiTullio, G.R., Mackey, D.J., 2000. Iron and manganese in the Ross

630 Sea, Antarctica: seasonal iron limitation in Antarctic shelf waters. J Geophys Res 105,

631 11321-11336.

632 Sedwick, P.N., Garcia, N.S., Riseman, S.F., Marsay, C.M., DiTullio, G.R., 2007.

633 Evidence for high iron requirements of colonial *Phaeocystis antarctica* at low

634 irradiance. Biogeochemistry 83, 83-97.

635 Sedwick, P.N., Marsay, C.M., Sohst, B.M., Aguilar-Islas, A.M., Lohan, M.C., Long,

636 M.C., Arrigo, K.R., Dunbar, R.B., Saito, M.A., Smith, W.O., Jr., DiTullio, G.R.,

637 2011. Early season depletion of dissolved iron in the ross Sea polynya: implications

638 for iron dynamics on the Antarctic continental shelf. J Geophys Res 116, C12019.

639 Shi, T., Sun, Y., Falkowski, P.G., 2007. Effects of iron limitation on the expression of

640 metabolic genes in the marine cyanobacterium *Trichodesmium erythraeum* IMS101.

641 Environmental Microbiology 9, 2945-2956.

642 Smith, W.O.J., Asper, V.A., Tozzi, S., Liu, X., Stammerjohn, S.E., 2011. Surface

643 layer variability in the Ross Sea, Antarctica as assessed by in situ fluorescence

644 measurements. Progress in Oceanography 88, 28-45.

645 Smith, W.O.J., Dennett, M.R., Mathot, S., Caron, D.A., 2003. The temporal dynamics

646 of the flagellated and colonial stages of Phaeocystis antarctica in the Ross Sea. Deep-

647 Sea Research II 50, 605-617.

648 Smith, W.O.J., Dinniman, M.S., Hoffman, E.E., Klinck, J.M., 2014. The effects of

649 changing winds and temperatures on the oceanography of the Ross Sea in the 21st

650 century. Geophysical Research Letters 41, 1624-1631.

651 Smith, W.O.J., Dinniman, M.S., Tozzi, S., DiTullio, G.R., Mangoni, O., Modigh, M.,

652 Saggiomo, V., 2010. Phytoplankton photosynthetic pigments in the Ross Sea: Patterns

653 and relationships among functional groups. Journal of Marine Systems 82, 177-185.

654 Smith, W.O.J., Dunbar, R.B., 1998. The relationship between new production and

655 vertical flux on the Ross Sea continental shelf. Journal of Marine Systems 17, 445-

656 457.

657   Smith, W.O.J., Gordon, L.I., 1997. Hyperproductivity of the Ross Sea (Antarctica)

658   polynya during austral spring. Geophysical Research Letters 24, 233-236.

659   Smith, W.O.J., Jones, R.M., 2015. Vertical mixing, critical depths, and phytoplankton

660   growth in the Ross Sea. ICES J Mar Sci 72, 1952-1960.

661   Smith, W.O.J., Marra, J., Hiscock, M.R., Barber, R.T., 2000. The seasonal cycle of

662   phytoplankton biomass and primary productivity in the Ross Sea, Antarctica. Deep-

663   Sea Research II 47, 3119-3140.

664   Smith, W.O.J., Shields, A.R., Peloquin, J.A., Catalano, G., Tozzi, S., Dinniman, M.S.,

665   Asper, V.A., 2006. Interannual variations in nutrients, net community production, and

666   biogeochemical cycles in the Ross Sea. Deep-Sea Research II 53, 815-833.

667   Strzepek, R.F., Harrison, P.J., 2004. Photosynthetic architecture differs in coastal and

668   oceanic diatoms. Nature 431, 689-692.

669   Strzepek, R.F., Hunter, K.A., Frew, R.D., Harrison, P.J., Boyd, P.W., 2012. Iron-light

670   interactions differ in Southern Ocean phytoplankton. Limnol Oceanogr 57, 1182-

671   1200.

672   Strzepek, R.F., Maldonado, M.T., Hunter, K.A., Frew, R.D., Boyd, P.W., 2011.

673   Adaptive strategies by Southern Ocean phytoplankton to lessen iron limitation:

674   Uptake of organically complexed iron and reduced cellular iron requirements. Limnol

675   Oceanogr 56, 1983-2002.

676   Suggett, D.J., Moore, C.M., Hickman, A.E., Geider, R.J., 2009. Interpretation of fast

677   repetition rate (FRR) fluorescence: signatures of phytoplankton community structure

678   versus physiological state. Mar Ecol Prog Ser 376, 1-19.

679   Sunda, W.G., Huntsman, S.A., 1997. Interrelated influence of iron, light and cell size

680   on marine phytoplankton growth. Nature 390, 389-392.

681   Tagliabue, A., Arrigo, K.R., 2003. Anomalously low zooplankton abundance in the

682   Ross Sea: An alternative explanation. Limnol Oceanogr 48, 686-699.

683   Tagliabue, A., Arrigo, K.R., 2005. Iron in the Ross Sea: 1. Impact on CO2 fluxes via

684   variation in phytoplankton functional group and non-Redfield stoichiometry. J

685   Geophys Res 110, C03009.

686   Tagliabue, A., Bopp, L., Aumont, O., 2008. Ocean biogeochemistry exhibits

687   contrasting responses to a large scale reduction in dust deposition. Biogeosciences 5,

688   11-24.

689   Welschmeyer, N.A., 1994. Fluorometric analysis of chlorophyll-*a* in the presence of

690   chlorophyll-b and pheopigments. Limnol Oceanogr 39, 1985-1992.

691   Wu, H., Cockshutt, A.M., McCarthy, A., Campbell, D.A., 2011. Distinctive

692   Photosystem II Photoinactivation and Protein Dynamics in Marine Diatoms. Plant

693   Physiology 156, 2184-2195.

694

695   **Tables and Fig. Legends**

696

697   **Table 1** Locations for long-term experiments conducted during NBP12-01 along with values

698   of initial F_v/F_m, $\Delta(F_v/F_m)$ (Equation 1), net growth rates estimated from chlorophyll

699   accumulation (Supplementary Information, Equation S1) and nitrate drawdown

700   (Supplementary Information, Equation S2) over 168 h. Shown are averages ± standard errors

701   (n = 3 or 5), * indicate significant differences (Two-way ANOVA, *p*<0.05) from control.

702

703   **Fig. 1 Composite map of Southern Ocean MODIS chlorophyll *a* for December 2011 –**

704   **February 2012. Inset:** Long-term (blue dots) and short-term (red dots) experimental locations

705   conducted on cruise NBP12-01 in the Ross Sea with 250 m bathymetric contours. Surface *in*

706   *situ* samples were also collected at these locations and at those marked CTD-station (black

707   dots).

708

709   **Fig. 2** Surface chlorophyll concentrations (μg L^{-1}) from CTD stations **(a)**. Surface DIN

710   concentrations (μM) **(b)**. Surface F_v/F_m **(c)**. Surface DFe concentrations (nM) **(d)**. Chlorophyll,

711   DIN and F_v/F_m from samples collected at 1-5 m depth, DFe from samples collected at ~10 m

712   depth.

713

714   **Fig. 3** Matrix of Pearson's linear correlation coefficients between the variables measured in the

715   surface waters of the Ross Sea, including: sea surface temperature (SST), Nitrate (DIN),

716   Phosphate (PO_4^{3-}), Silicate (Si), community structure (% Diatoms), chlorophyll concentration,

717   F_v/F_m, σ_{PSII}, F_m:PsbA, Chl:PsbA, and dissolved iron concentrations (DFe). The strength of the

718   linear association between each pair of variables is indicated by the colour of the square, with

719   the negative and positive correlations denoted by '-' and '+' within all squares where

720   significant (p<0.01).

721

722   **Fig. 4** Spatial distribution of $\Delta(F_v/F_m)$ calculated from Fe addition incubation experiments **(a)**.

723    $\Delta(F_v/F_m)$ calculated from long-term Fe-addition incubation experiments in the Ross Sea, both

724   from (1) near the Ross Ice Shelf, (2) over the Ross Bank and (3) within an anti-cyclonic eddy

725   **(b)**. The change in chlorophyll normalized maximum fluorescence, (ΔF_m Chl^{-1}) from the three

726   long-term Fe addition incubation experiments **(c)**. The change in chlorophyll normalized

727   variable fluorescence $\Delta(F_v$ Chl$^{-1})$ from the three long-term Fe addition incubation experiments

728   **(d)**. Shown are averages with ± standard errors (*n* = 4 or 5). * represent statistically significant

729   differences (*t-test*, *p<0.05*).

730

731   **Fig. 5** Relationship of DIN (μM) and photosynthetic efficiency (F_v/F_m) throughout the Ross

732   Sea as a function of a) chlorophyll concentrations (μg L^{-1}), b) phytoplankton composition (%),

733   and c) the relative degree of Fe stress Δ(F_v/F_m) **(c)**. Grey dots represent stations where DIN and

734   F_v/F_m were measured but no corresponding additional variables were measured.

735

736   **Fig. 6** Relationship of DIN (μM) and photosynthetic efficiency (F_v/F_m) throughout the Ross

737   Sea as a function of a) functional cross-section of photosystem II (σ_{PSII}) (nm^{-2}), b) the ratio of

738   chlorophyll to PsbA (a core subunit of PSII) (mmol mol^{-1}), c) the ratio of the maximum

739   fluorescence yield to chlorophyll (F_m:Chl), and d) the ratio of the maximum fluorescence yield

740   to PsbA (F_m:PsbA). Grey dots represent stations where DIN and F_v/F_m were measured but no

741   corresponding additional variables were measured.
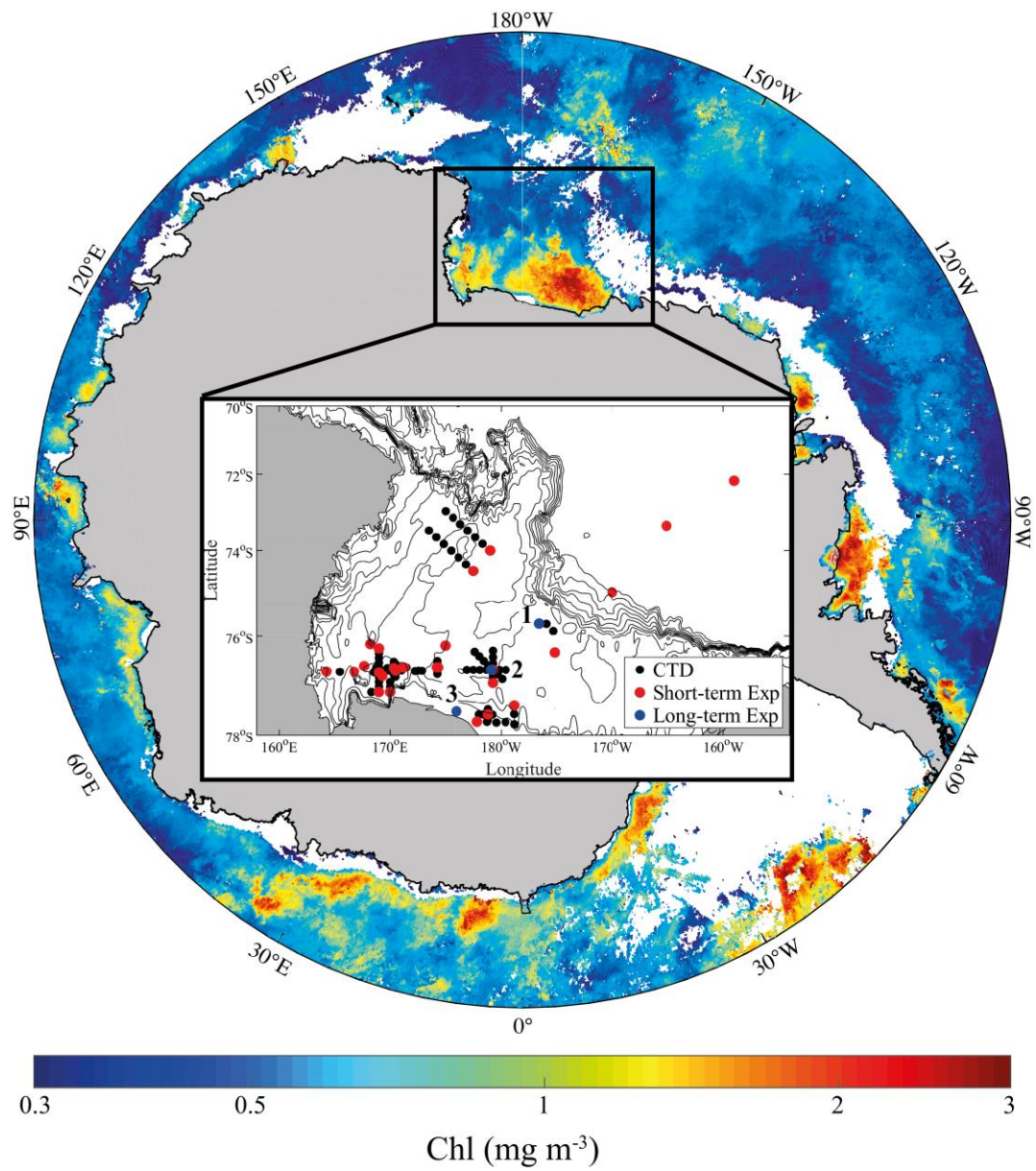
742

743   Table 1

744

Experiment	1	2	3
Lat (°S)	75.72	76.72	77.55
Long (°W)	183.40	179.08	175.97
$F_v/F_{m\ Initial}$	0.26 ±0.01	0.29 ±0.00	0.21 ±0.00
$\Delta (F_v/F_m)$, 24 h	0.04 ±0.01	0.00 ±0.00	0.01 ±0.00
$\mu_{Control}^{Chl}$ (d⁻¹), 0 -168 h	0.11 ±0.02	0.25 ±0.01	0.13 ±0.01
μ_{Fe}^{Chl} (d⁻¹), 0 -168 h	0.17* ±0.02	0.29* ±0.00	0.19* ±0.01
ΔNO_3^- Control (μ M d⁻¹), 0 – 168 h	1.61 ±0.33	1.50 ±0.04	2.43 ±0.08
ΔNO_3^- Fe (μ M d⁻¹), 0 – 168 h	2.53* ±0.13	1.57 ±0.05	2.93* ±0.07

745

746   Fig. 1

747

748

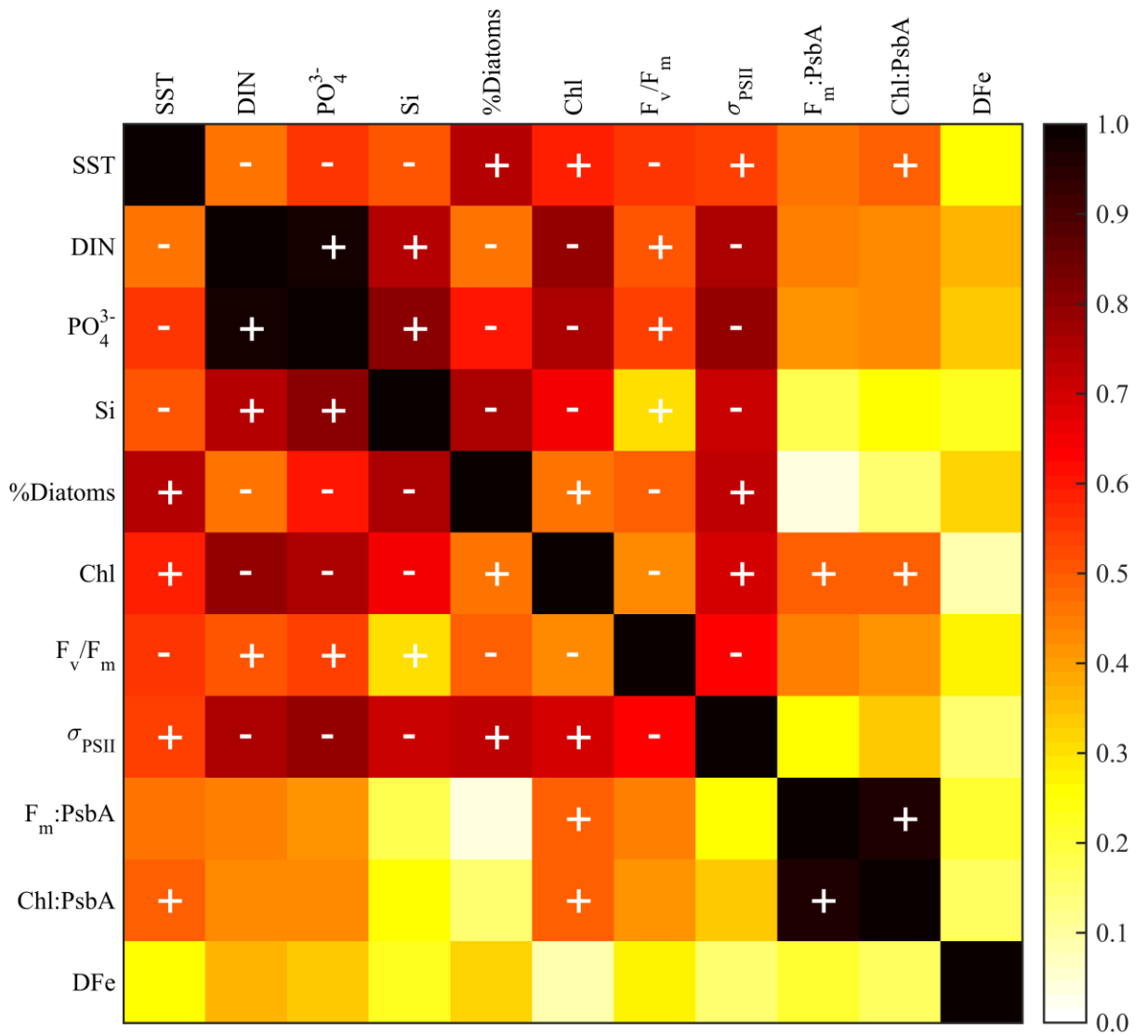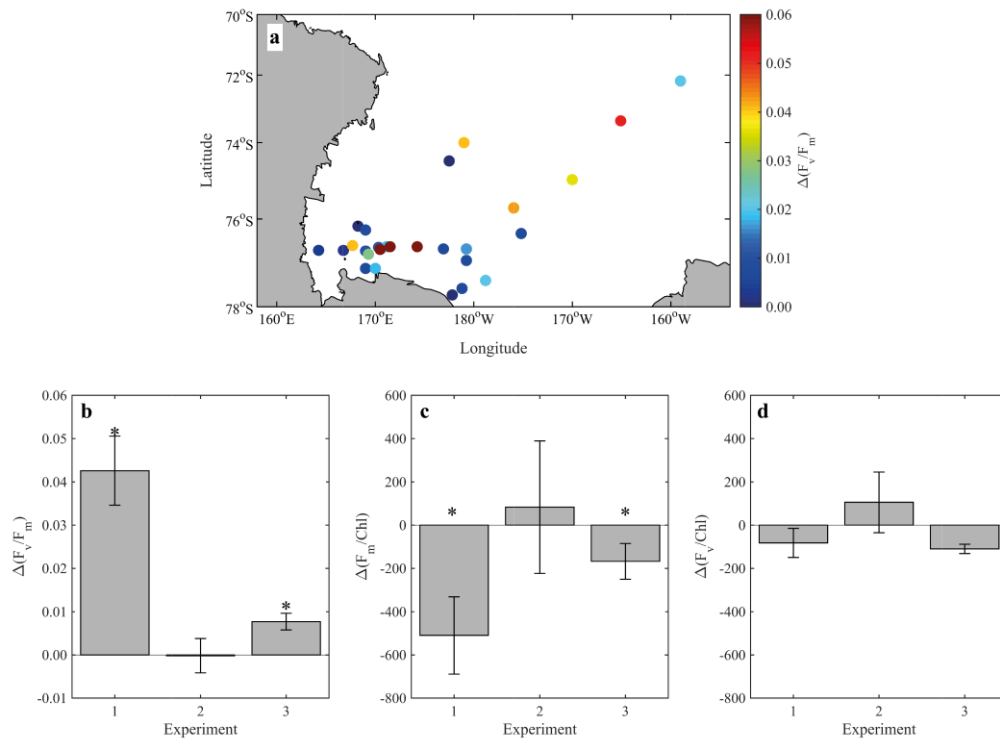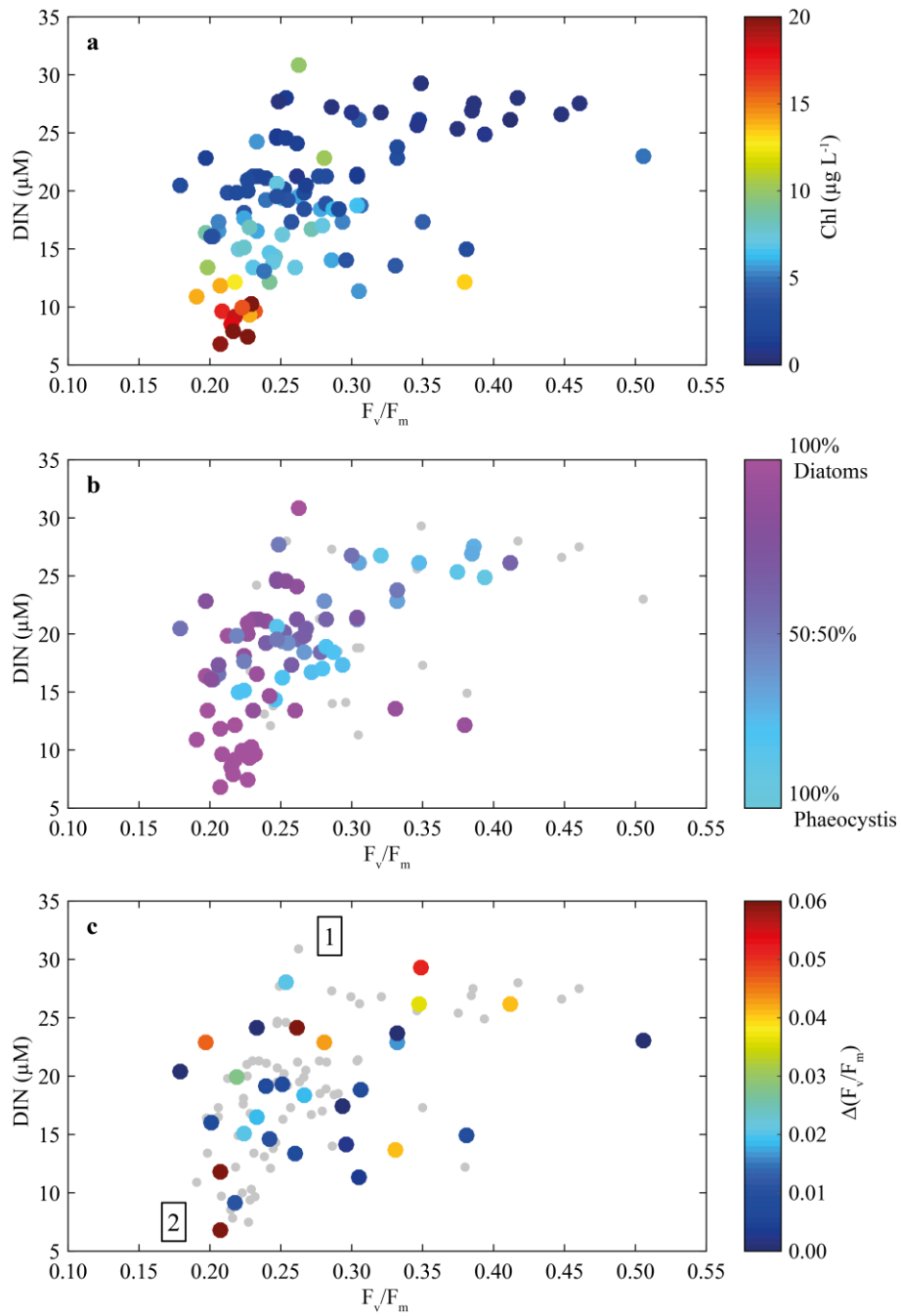749   Fig. 2

750

751
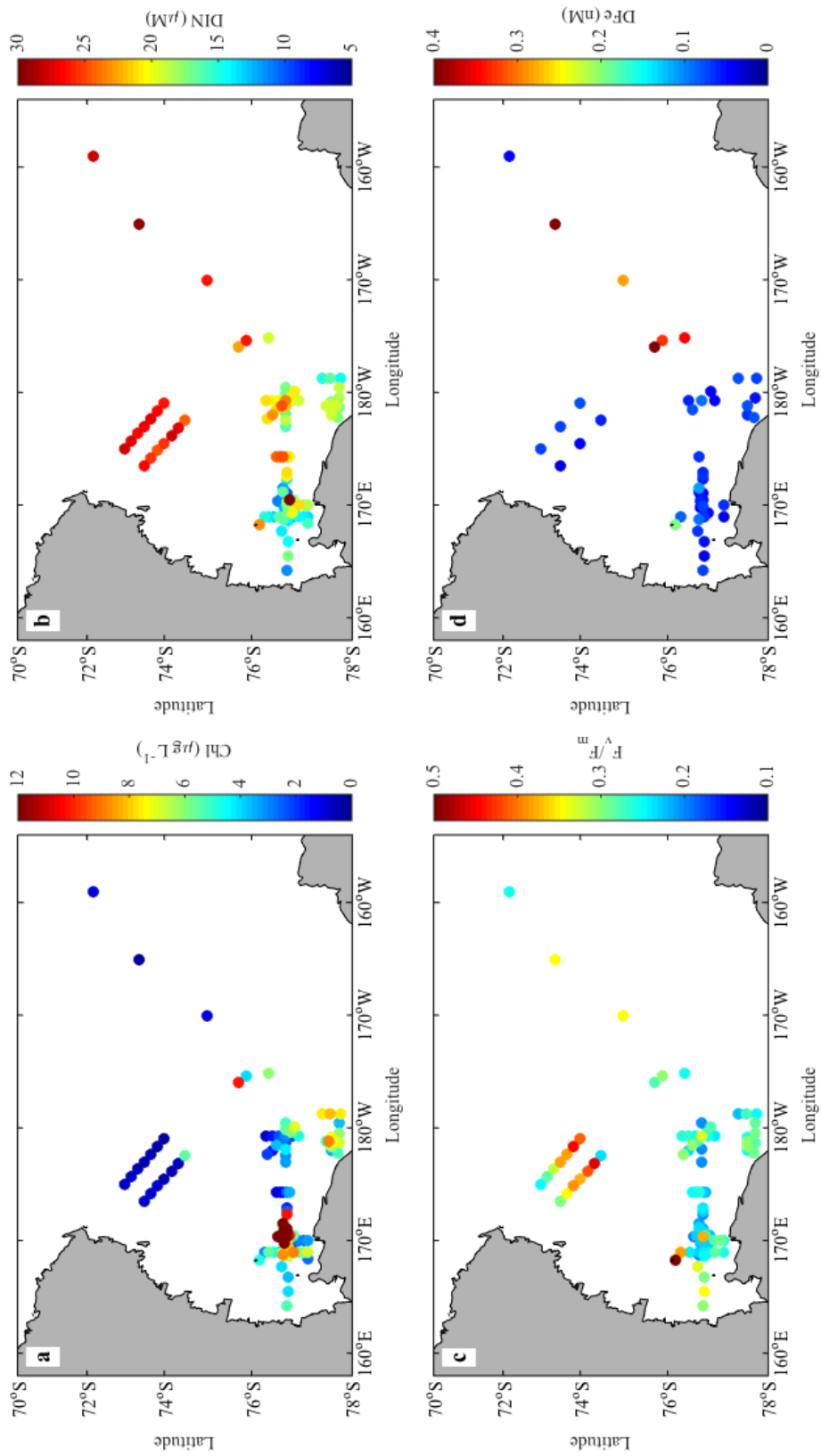
752   Fig. 3

753
754

755   Fig. 4

756
757

758　　　Fig. 5

759
760

761   Fig. 6

762